Biallelic variants in *ADAMTS15* cause a novel form of distal arthrogryposis

Felix Boschann, Muhsin Ö. Cogulu, Davut Pehlivan, Saranya Balachandran, Pedro Vallecillo-Garcia, Christopher M. Grochowski, Nils R. Hansmeier, Zeynep H. Coban Akdemir, Cesar A. Prada-Medina, Ayca Aykut, Björn Fischer-Zirnsak, Simon Badura, Burak Durmaz, Ferda Ozkinay, René Hägerling, Jennifer E. Posey, Sigmar Stricker, Gabriele Gillessen-Kaesbach, Malte Spielmann, Denise Horn, Knut Brockmann, James R. Lupski, Uwe Kornak, and Julia Schmidt

Supplemental Data

Content

Supplemental Material and Methods:

Participants

Parental consent was obtained for all clinical and molecular studies of this report and for the publication of clinical photographs. The study was performed in accordance with the Declaration of Helsinki protocols and approved by the Ethics Committee of University Medical Center Göttingen (approval # 3/2/16 – Family A and C), Baylor College of Medicine IRB (approval # H29697 – Family B =HOU1335=BH2122) and Charité – Unversitätsmedizin Berlin (approval # EA2/166/20 – Family D).

Exome Sequencing/ Panel Sequencing

For families A and D, genomic DNA was isolated from peripheral blood and enriched with a SureSelect Human All Exon Kit V6 (Agilent technologies, Santa Clara, California) for subsequent Trio-ES on an Illumina system (Illumina, San Diego, California). Reads were aligned to human genome build GRCh37/hg19. Sequence reads were called and analyzed according to an in-house standard operating procedure using the VarFish platform.[1] In brief, variants were filtered by minor allele frequency, mode of inheritance, predicted functional impact (i.e., missense, nonsense, splicing). In family D, we specifically searched for variants in *ADAMTS15* and already known DA genes (Genomics England PanelApp: Arthrogryposis v3.122).

For family B (BAB3440) ES was performed at Baylor College of Medicine Human Genome Sequencing Center through the Baylor-Hopkins Center for Mendelian Genomics research initiative. For variant prioritization, we used external publicly-available databases such as the 1000 Genomes Project and other large-scale sequencing projects including gnomAD, the Exome variant server, NHLBIGO Exome Sequencing Project (ESP), and the Atherosclerosis Risk in Communities Study (ARIC) Database, and our “in-house-generated” exomes (from over 13,000 individuals) at

Baylor College of Medicine Human Genome Sequencing Center. All experiments and analyses were performed according to previously described methods.[2] Briefly, samples underwent exome capture using Human Genome Sequencing Center core design (52Mb, Roche NimbleGen), followed by sequencing on the HiSeq platform (Illumina, Inc) with an average depth-of-coverage of 115X and 90.03% of bases covered at >20X. Sequence data were aligned and mapped to the human genome reference sequence (hg19) using the Mercury in-house bioinformatics pipeline. Variants were called using the ATLAS (an integrative variant analysis pipeline optimized for variant discovery) and the Sequence Alignment/Map (SAMtools) suites and annotated with an in-house-developed annotation pipeline that uses Annotation of Genetic Variants (ANNOVAR) and additional tools and databases.[3-5]

Variant detection in family C occurred via a custom gene panel (SureSelect) (Agilent technologies, Santa Clara, California) and sequencing using a NextSeq sequencer (Illumina, San Diego, California). Alignment, variant calling, and prioritization was done using the SeqNext software (JSI medical systems, Ettenheim, Germany). Variants were classified according to the ACMG/AMG criteria.[6] Collaborators were connected through GeneMatcher.[7]

Absence of Heterozygosity (AOH) Calculation

We detected runs of homozygosity (ROH) regions from unphased ES data as absence of heterozygosity (AOH) genomic intervals with BafCalculator (https://github.com/BCM-Lupskilab/BafCalculator).[8] VCF files were used to identify regions of ROH using the following algorithm: first, from all SNVs that passed quality filters in the single VCF, we extracted a B-allele frequency (i.e., variant reads/total reads ratio); next, we transformed this ratio by subtracting 0.5 and taking the absolute value for each data point. After such a transformation, values > 0.47 were considered

indicative of homozygous or hemizygous variants (expected value is 0.5) corresponding to either alternative or reference alleles, whereas lower values likely indicate heterozygous alleles. Transformed B-allele frequency data were then processed using Circular Binary Segmentation (CBS) implemented in the DNAcopy R Bioconductor package.[9,10] In summary, segments with the mean signal > 0.47 and number of marks >= 10 were classified as ROH regions.

Splice site analysis via ddPCR and RT-PCR

Primary fibroblasts from affected individual 3 (BAB3440) and healthy control subjects were cultivated. RNA was extracted from all samples at three timepoints using Trizol adapted protocols. cDNA was synthesized separately using the BioRad iScript cDNA synthesis. Standardized 100 ng cDNA was used for each reaction. To investigate the impact of the splice variant identified in BAB3440, ddPCR was performed on a Bio-Rad QX200 system. Two independent TaqMan probes that used a distinct fluorescent tag were designed to selectively amplify only in the presence of exon 7 (FAM tag, sitting at the exon6-exon7 junction) with a control probe (HEX tag). The assay was run with a QX200 AutoDG ddPCR system from Bio-Rad according to normal protocols for a TaqMan reaction. Individual positive droplet populations for both fluorescent probes were quantified with the QuantaSoft software suite from Bio-Rad. Standard protocols were used for amplification of *ADAMTS15* exons 6 to 8 on cDNA level and subsequent Sanger sequencing.

Protein structure visualization

The 3D structure model for ADAMTS15 was predicted by AlphaFold and obtained through https://alphafold.ebi.ac.uk/.[11]

In situ hybridization

The probe used for *Adamts15* detection in whole mount *in situ* hybridization (WISH) was previously developed by the Eurexpress consortium, the probe used for *Osr1* was described before.[12,13]

Whole mount *in situ* hybridization was performed as previously described.[14] In brief, digoxigenin-labeled cRNA probes were generated from the PCR product according to manufacturer's instructions (Roche Life Science, Mannheim, Germany). Embryos were washed in PBS and fixed overnight at 4°C in 4% paraformaldehyde. Embryos were pretreated with proteinase K (10 µg/ml) and hybridized overnight at 65°C in a buffer containing 50% formamide. After washing, the embryos were incubated with the DIG antibody (Roche Life Science, Mannheim, Germany) at a dilution of 1:5000 at 4°C overnight. After washing in TBST buffer, staining was performed at room temperature (RT) for up to 4 h or overnight at 4°C.

Section *in situ* hybridization (ISH) was performed essentially as described before.[15] In brief, 10 µm cryosections of PFA-fixed mouse embryos were treated with acetylation buffer (0.75% triethanolamine, 0.15% hydrogen chloride and 0.2% acetic anhydride in DEPC-H2O) for 10 min and hybridized overnight at 65°C in a buffer containing 50% formamide. After several washes with 2x SSC and blocking (MABT-buffer + 5% blocking reagent, Roche Life Science, Mannheim, Germany), slides were incubated with anti-DIG antibody (Roche Life Science, Mannheim, Germany) at a dilution of 1:2000 at 4°C overnight. After washing, staining was performed using NBT (75 mg/ml) and BCIP (50 mg/ml). Sections were incubated with pan-anti-myosin heavy chain antibody (Clone A4.1025) (Merck Chemicals GmbH, Darmstadt, Germany) at 4 °C overnight, followed by secondary antibody staining of 1 h at room temperature.

RNAscope expression analysis

Simultaneous RNA *in situ* hybridization was performed using the RNAscope® technology (Advanced Cell Diagnostics [ACD], Newark, CA, USA) and the following probes specific for Mm-Adamts15 (Cat. No. 840941, ACD) and Mm-Osr1 (Cat. No. 496281-C2, ACD) on five µm sections of PFA-fixed mouse embryos. RNAscope probes were purchased by ACD and designed as described by Wang et al.,.[16] The RNAscope® assay was run on a HybEZ™II Hybridization System (Cat. No. 321720, ACD) using the RNAscope® Multiplex Fluorescent Reagent Kit v2 (Cat. No. 323100, ACD) and the manufacturer's protocol for fixed-frozen tissue samples with target retrieval on a hotplate for 5 min. Fluorescent labeling of the RNAscope® probes was achieved by using OPAL 520 and OPAL 570 dyes (Cat. No. FP1487001KT + Cat. No. FP1488001KT, Akoya Biosciences, Marlborough, MA, USA) and stained sections were scanned at 25x magnification using a LSM 980 with Airyscan 2 (Carl Zeiss AG, Oberkochen, DE).

Single-cell RNA sequencing/ trajectory analysis

Whole embryo single-cell mesenchymal trajectory that was preprocessed was downloaded from Mouse Organogenesis Cell Atlas (MOCA).[17] Monocle3 was used for the further analysis.[18] The data was preprocessed, dimensionally reduced and clustered using the default parameters of monocle3. Expression of genes of interest was visualized used the plot cells function of monocle3.

Single-cell RNA fastq files for mouse forelimb dataset were obtained from ENCSR713GIS[19] for the timepoints E10.5 to E15.0 and for hindlimb from GSM4227224[20] for the timepoints E11.5 to E18.5.[21] From the fastq files, a gene-barcode UMI count matrix was generated per sample using the CellRanger count pipeline v.3.0 (10X Genomics) using default parameters for the both datasets. Scrublet

was used to estimate the doublets where cells with a doublet score below 0.2 were retained for the analysis.[22] Seurat v3 was used for the downstream analysis. Cells with more than 1000 UMI and 500 genes and less than 10% mitochondrial DNA and 60% of ribosomal genes content were retained. We also filtered out the ribosomal and mitochondrial genes. Samples were normalized and scaled using the SCTransformation approach.[23] The samples were then integrated to facilitate inter-sample comparisons using the reciprocal PCA approach in Seurat, based on the top 1000 most variable genes and their top 50 principal components.[24] The cells were clustered using Louvain clustering algorithm based on nearest neighbors' graph build using the sample-corrected 50 PCA components (resolution of 0.05). Differential expression analysis was then carried out using ROC statistical test to identify the cell types, where the parameters such as, average fold change and percentage of cells expressing the gene per cluster, greater than 0.25 were used to restrict the number of identified DE genes. Differential expression of well-known marker genes for the main limb cellular lineages were used to name the identified cell clusters. Cells co-expressing the genes of interest were plotted using FeaturePlot function of Seurat.

Supplemental Clinical Information

Family A

Individual 1 (II-1, Fig. 1)

The index individual II-1 was born at 32 weeks of gestation to healthy, consanguineous parents from Syria. His exact birth parameters are not known. Contractures of the hands and bilateral talipes equinovarus were noted shortly after delivery. He had surgical extension of the Achilles tendon at the age of two years. At his last clinical evaluation at age 17 years and 5 months, he had a height of 163.5 cm (- 2.3 SD) and a weight of 67.0 kg (- 0.3 SD). He showed contractures of the finger and toe joints with absent palmar creases in the distal interphalangeal region. He was not able to clench his fist and reported problems in grasping or carrying an object. He also had decreased flexibility of the lower spine and scoliosis. His pain-free walking distance was reduced to 500 meters. Additionally, he had tingling sensations in the legs at rest combined with the urge to move. The affected individual reported no progression of symptoms. Electromyography (EMG) and nerve conduction velocity (NCV) were unremarkable. His cognitive development was normal. Except strabismus, slightly low-set ears and dental crowding, he showed no facial dysmorphism. Vision and hearing appeared to be normal and there were no signs of cardiovascular abnormalities. Radiographs of the hands and genetic testing including array CGH analysis and Sanger sequencing of *NOG* and *GDF5* were unremarkable.

Individual 2 (II-4, Fig. 1)

His affected brother, individual 2, was born at term by C-section. His exact birth parameters are unknown. At birth, he presented with contractures of the hands and feet. Clinical examination at the age of 9 years and 7 months revealed a height of 129

cm (- 1.7 SD), a weight of 26.4 kg (- 1.4 SD) and a head circumference of 51 cm (- 1.9 SD). He showed non-progressive contractures of the finger joints and absent distal phalangeal creases similar to his affected brother (II-1). Grasp and pinch functions were impaired. He had surgical extension of the Achilles tendon at the age of 9 years. Otherwise, his feet seemed to be less affected than his brother's (II-1) (Supplemental Figure 1). He had not developed acroparesthesia. He also showed spinal rigidity, scoliosis, dental crowding and slightly low set ears. His cognitive development and radiographs of the hands (Supplemental Figure 1) were unremarkable. There were no signs of ophthalmological or cardiovascular abnormalities.

In individual 1, Trio-ES identified a homozygous stop-gain variant in exon 1 of *ADAMTS15* c.123C>G, p.(Tyr41*) [NC_000011.9:g.130318991C>G; NM_139055.3; NP_620686.1]. The unaffected parents are heterozygous for the variant. This alteration has not been described previously and is absent from gnomAD (v.2.1.1). Sanger sequencing confirmed homozygosity for the variant in the affected brother (individual 2, II-4). The unaffected siblings (II-2, II-3, II-5) do not carry the variant in homozygous state (Figure 2A, Supplemental Figure S4). Total autosomal AOH in the proband was 360.5 Mb and the variant was located within a 5.3 Mb long AOH block.

Family B

Individual 3 (II-6, Fig. 1)

Individual 3 (II-6, Figure 1) was born to consanguineous parents from Turkey at term via normal spontaneous vaginal delivery after an uncomplicated pregnancy. Her birth weight was 3,000 g (- 1.1 SD), height was 50 cm (- 0.8 SD) and head circumference was 35 cm (+ 0.1 SD). Her developmental milestones were normal. She had absent palmar creases especially in the interphalangeal region, flexion contractures in the

PIPs of both hands, and contractures in all toes. There were no erosions over the joints. Furthermore, she gradually developed dry and stiff skin in the upper and lower extremities. She was being followed by Dermatology with a diagnosis of “scleroderma” after a skin biopsy. She had no difficulties in swallowing, gastroesophageal reflux or morning stiffness. Scleroderma autoantibodies, metabolic screening tests, complete blood count, comprehensive metabolic panel, lactic acid and pyruvic acid were within normal ranges. Abdominal ultrasound, esophageal passage radiograph and lung high-resolution CT were unremarkable. Echocardiography showed mitral valve prolapse. Her pains particularly in the lower extremities presented with intermittent cramps, which were not increasing by movement. Stiffness in the hands, feet and back were limiting her daily life. She was started on methotrexate, methyl prednisolone and folic acid with no improvement in symptoms.

She had a history of surgery for inguinal hernia at 5 years of age. Additionally, she was found to have subchondral cyst in the knee and wrists, which were subsequently surgically removed. A meniscal tear was repaired during the same procedure. Dual energy X-ray absorptiometry revealed osteoporosis. Anthropometric measurements at the age of 17 years were as follows: weight: 47 kg (- 1.7 SD), height: 165 cm (- 0.5 SD) and head circumference was 56 cm (+ 0.6 SD). On physical examination, she had low-set ears, hypertelorism, epicanthus, long philtrum, absence of two teeth (Supplemental Figure 1), camptodactyly and flexion contractures in both hands and feet. She reported excessive sweating in the palms and distal cyanosis particularly during exposure to cold,

In family B (HOU1335), ES detected the homozygous intronic variant c.1903-2A>G in individual 3 (BAB3440). Bioinformatic *in silico* predictions indicated loss of function of the authentic acceptor splice site. The variant was heterozygous in both parents and

the unaffected sister (Figure 1A, Supplemental Figure 4). The variant is absent from gnomAD v2.1.1. The variant was located within a 4.1 Mb large AOH block.

Since *ADAMTS15* expression is almost absent in skin fibroblasts or leukocytes we had to use the highly sensitive droplet digital RT-PCR for analyzing the effect of the intronic variant found in affected individual 3. Using a probe specific for the exon 6/7 junction a complete loss of signal was observed compared to mRNA from skin fibroblasts from healthy controls (Supplemental Figure 2A,B). Sanger sequencing of the cDNA amplicon showed that the variant c.1903-2A>G causes a complete skipping of exon 7 (r.1903_2078del), which is predicted to result in a frameshift and premature stop of translation p.(Val635Alafs*30) (Supplemental Figure 2C).

Family C

Individual 4 (II-1, Fig. 1)

Individual 4 was born at 40 weeks of gestation to healthy, consanguineous parents from Kosovo. Birth weight was 3,460 g (- 0.4 SD), length 51 cm (- 0.7 SD) and OFC 34 cm (- 1.2 SD). He had inguinal hernia surgery and orchidopexy at the age of 1 year. He suffered two pathological fractures and received genetic testing for osteogenesis imperfecta, which was unremarkable. His psychomotor development was normal. At age 3 years and 1 month, his height was 96.2 cm (- 0.3 SD), weight 14.0 kg (- 0.4 SD), and OFC was 50.2 (- 0.4 SD). He showed no signs of ophthalmological or cardiovascular abnormalities.

We detected the homozygous missense variant c.221G>A, which is predicted to result in the p.(Gly761Ser) substitution. The parents are heterozygous for the variant. The variant has a CADD score (v.1.6) of 28.9 and affects a highly conserved amino acid residue within the ADAMTS spacer 1 domain of the ADAMTS15 protein. The variant is listed once in gnomAD (v.2.1.1.) in a heterozygous state but not in a homozygous state.

Family D

Individual 5 (II-2, Fig. 1)

Individual 5 was born in Germany to unaffected consanguineous parents of Turkish ancestry. Prenatal ultrasound demonstrated oligohydramnios. In addition, the mother reported decreased fetal movement. He was delivered at term with normal measurements and multiple congenital contractures, predominantly affecting the hands and feet. Postnatal adaption was complicated by feeding difficulties. He could sit at the age of 18 months and walk at 20 months of age. Fine motor development was delayed, and fine motor skills were still impaired at the age of 11 years due to distal joint contractures. Flexion contractures of the fingers and knees (Supplemental Figure 1) improved significantly with physiotherapy. Furthermore, left sided ptosis, reduced mouth opening, crowded teeth, kyphosis of the thoracic spine and pes planovalgus were noted. The ophthalmic evaluation showed visual impairment with hyperopia and strabismus. No other ophthalmological or any cardiovascular abnormalities have been noted. Recently, he underwent hydrocele surgery. At his last physical examination at 11 years of age, measurements were: height 123 cm (-1.6 SD), weight 21.6 kg (-3.1 SD), OFC 52.5 cm (-0.5 SD). Karyotyping, array CGH and targeted sequencing of *MYH8*, *RAPSN* and *FBN2* were unremarkable.

Trio-ES revealed homozygosity for the variant c.2715C>G in the affected child and heterozygosity in the unaffected parents. The variant is predicted to result in a p.(Cys905Trp) substitution at a highly conserved residue within the second thrombospondin type 1 repeat of the protein. The variant has a CADD score of 26.8 and is predicted to be damaging by different *in silico* tools (Mutation Taster, Polyphen-2, M-CAP). The variant is absent from gnomAD.

As in the other families, the variant occurred within a long-sized run of AOH (5.1 Mb).

Supplemental References:

1. Holtgrewe M, Stolpe O, Nieminen M, et al. VarFish: comprehensive DNA variant analysis for diagnostics and research. Nucleic Acids Res. 2020;48(W1):W162-W169.
2. Bainbridge MN, Hu H, Muzny DM, et al. De novo truncating mutations in ASXL3 are associated with a novel clinical phenotype with similarities to Bohring-Opitz syndrome. Genome medicine. 2013;5(2):11.
3. Challis D, Yu J, Evani US, et al. An integrative variant analysis suite for whole exome next-generation sequencing data. BMC bioinformatics. 2012;13:8.
4. Li H, Handsaker B, Wysoker A, et al. The Sequence Alignment/Map format and SAMtools. Bioinformatics. 2009;25(16):2078-2079.
5. Wang K, Li M, Hakonarson H. ANNOVAR: functional annotation of genetic variants from high-throughput sequencing data. Nucleic acids research. 2010;38(16):e164.
6. Richards S, Aziz N, Bale S, et al. Standards and guidelines for the interpretation of sequence variants: a joint consensus recommendation of the American College of Medical Genetics and Genomics and the Association for Molecular Pathology. Genet Med. 2015;17(5):405-424.
7. Sobreira N, Schiettecatte F, Valle D, Hamosh A. GeneMatcher: a matching tool for connecting investigators with an interest in the same gene. Hum Mutat. 2015;36(10):928-930.
8. Karaca E, Posey JE, Coban Akdemir Z, et al. Phenotypic expansion illuminates multilocus pathogenic variation. Genet Med. 2018;20(12):1528-1537.
9. Huber W, Carey VJ, Gentleman R, et al. Orchestrating high-throughput genomic analysis with Bioconductor. Nat Methods. 2015;12(2):115-121.
10. Olshen AB, Venkatraman ES, Lucito R, Wigler M. Circular binary segmentation for the analysis of array-based DNA copy number data. Biostatistics. 2004;5(4):557-572.
11. Jumper J, Evans R, Pritzel A, et al. Highly accurate protein structure prediction with AlphaFold. Nature. 2021;596(7873):583-589.
12. Diez-Roux G, Banfi S, Sultan M, et al. A high-resolution anatomical atlas of the transcriptome in the mouse embryo. PLoS Biol. 2011;9(1):e1000582.
13. Stricker S, Mathia S, Haupt J, Seemann P, Meier J, Mundlos S. Odd-skipped related genes regulate differentiation of embryonic limb mesenchyme and bone marrow mesenchymal stromal cells. Stem Cells Dev. 2012;21(4):623-633.
14. Schwabe GC, Trepczik B, Süring K, et al. Ror2knockout mouse as a model for the developmental pathology of autosomal recessive Robinow syndrome. Developmental Dynamics. 2004;229(2):400-410.
15. Vallecillo-Garcia P, Orgeur M, Vom Hofe-Schneider S, et al. Odd skipped-related 1 identifies a population of embryonic fibro-adipogenic progenitors regulating myogenesis during limb development. Nat Commun. 2017;8(1):1218.
16. Wang F, Flanagan J, Su N, et al. RNAscope: a novel in situ RNA analysis platform for formalin-fixed, paraffin-embedded tissues. J Mol Diagn. 2012;14(1):22-29.
17. Cao J, Spielmann M, Qiu X, et al. The single-cell transcriptional landscape of mammalian organogenesis. Nature. 2019;566(7745):496-502.

18. Trapnell C, Cacchiarelli D, Grimsby J, et al. The dynamics and regulators of cell fate decisions are revealed by pseudotemporal ordering of single cells. Nat Biotechnol. 2014;32(4):381-386.
19. He P, Williams BA, Trout D, et al. The changing mouse embryo transcriptome at whole tissue and single-cell resolution. Nature. 2020;583(7818):760-767.
20. Kelly NH, Huynh NPT, Guilak F. Single cell RNA-sequencing reveals cellular heterogeneity and trajectories of lineage specification during murine embryonic limb development. Matrix Biol. 2020;89:1-10.
21. Allou L, Balzano S, Magg A, et al. Non-coding deletions identify Maenli lncRNA as a limb-specific En1 regulator. Nature. 2021;592(7852):93-98.
22. Wolock SL, Lopez R, Klein AM. Scrublet: Computational Identification of Cell Doublets in Single-Cell Transcriptomic Data. Cell Syst. 2019;8(4):281-291 e289.
23. Hafemeister C, Satija R. Normalization and variance stabilization of single-cell RNA-seq data using regularized negative binomial regression. Genome Biol. 2019;20(1):296.
24. Stuart T, Butler A, Hoffman P, et al. Comprehensive Integration of Single-Cell Data. Cell. 2019;177(7):1888-1902 e1821.

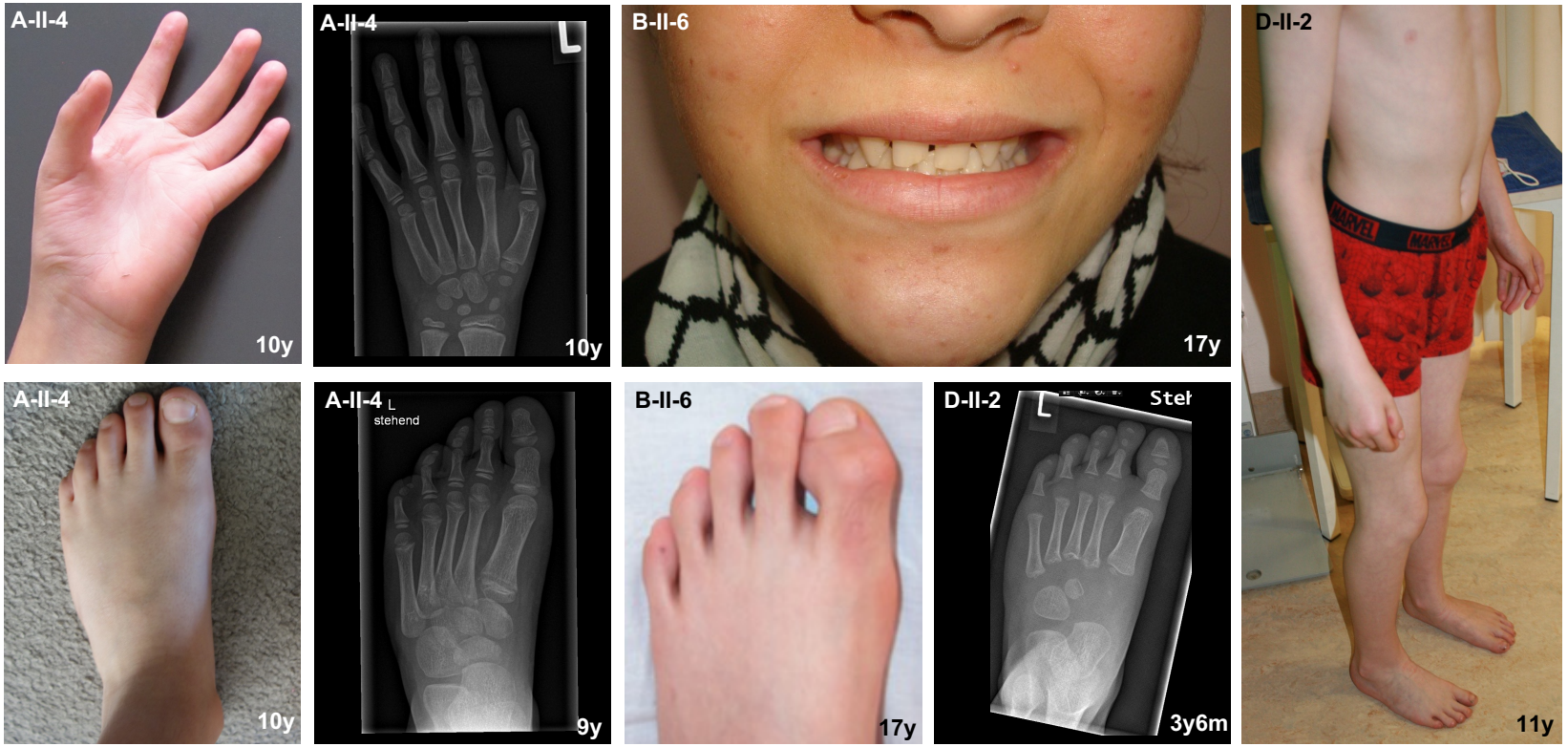

Figure S1. Additional phenotypic aspects.

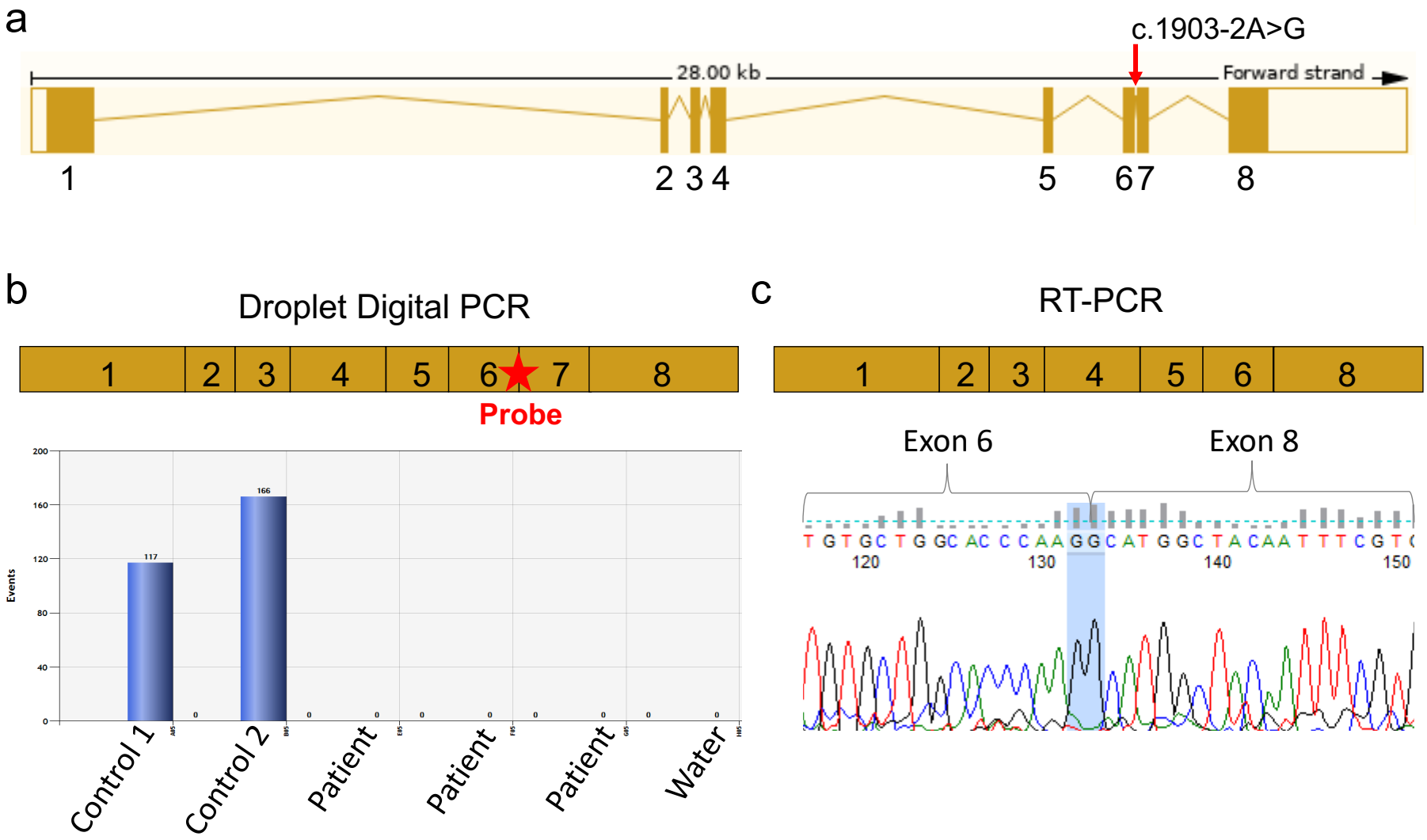

Figure S2. Splicing analysis. (a) Schematic overview of the *ADAMTS15* gene. (b) Localization of the intronic variant and the probe used for ddPCR at the junction between exon 6 and exon 7. ddPCR revealed no expression in skin fibroblasts of the affected individual 3 compared to controls. (c) Sanger sequencing of a cDNA amplicon confirmed skipping of exon 7 leading to the indicated transcript.

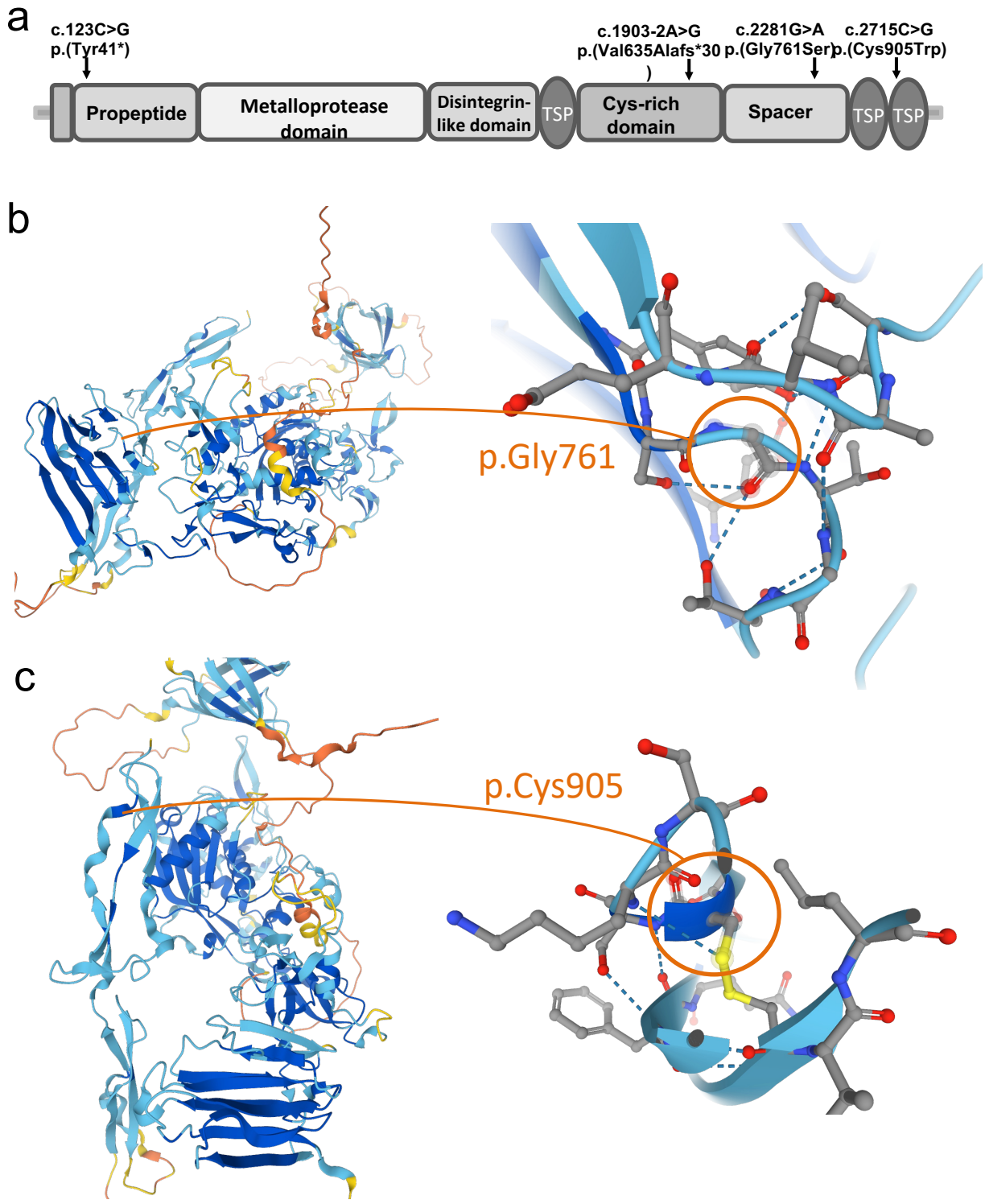

Figure S3. Structural modeling of missense variants c.2281G>A, p.(Gly761Ser) and c.2715C>G, p.(Cys905Trp). (a) Overview over ADAMTS15 domain structure. (b) Residue Gly761 forms hydrogen bonds and (c) Cys905 a disulfide bridge important for stability of the 3D structure.

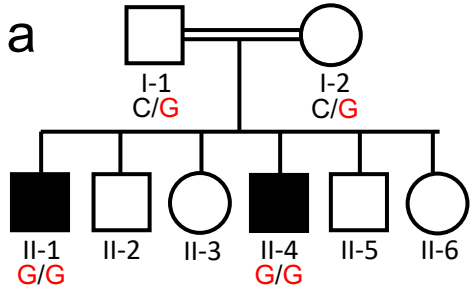

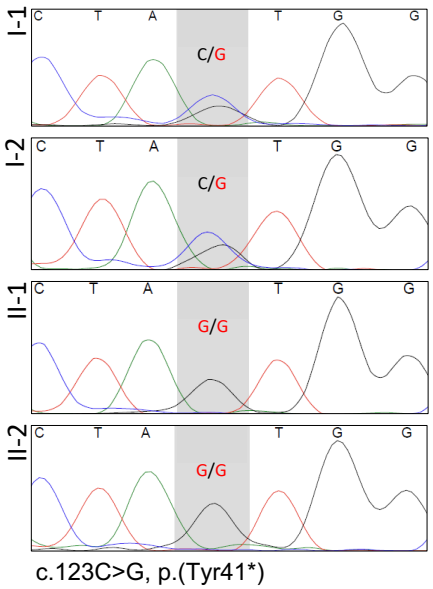

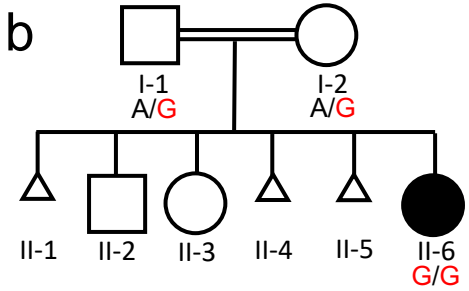

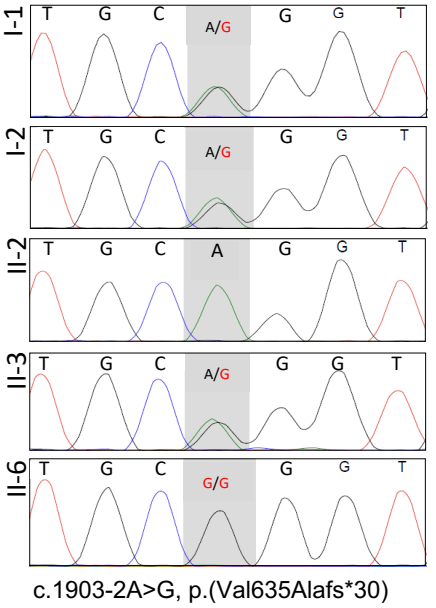

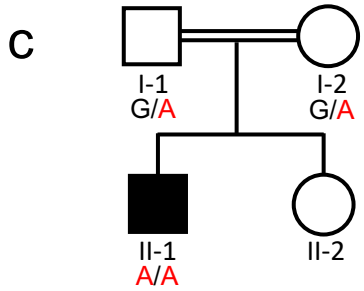

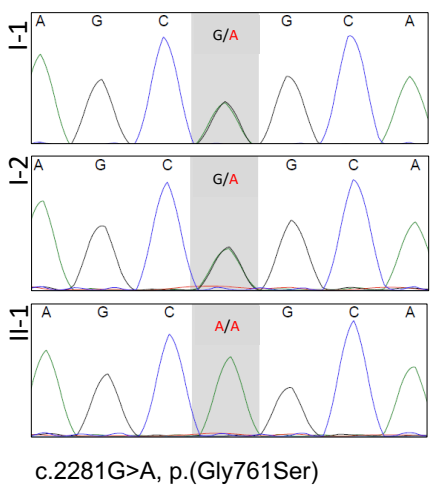

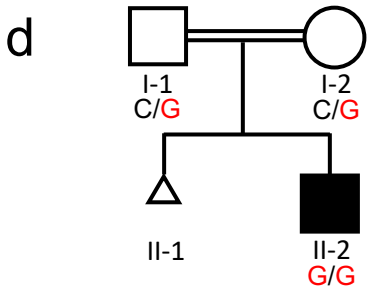

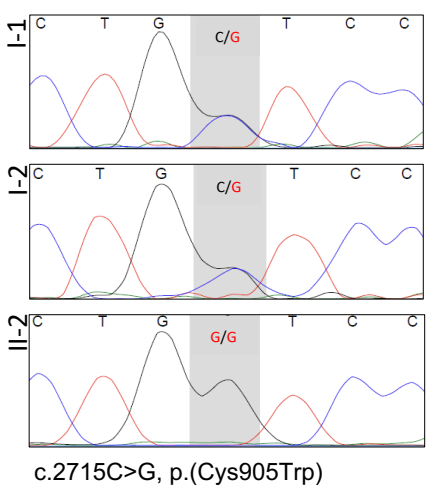

Figure S4. Segregation analysis.

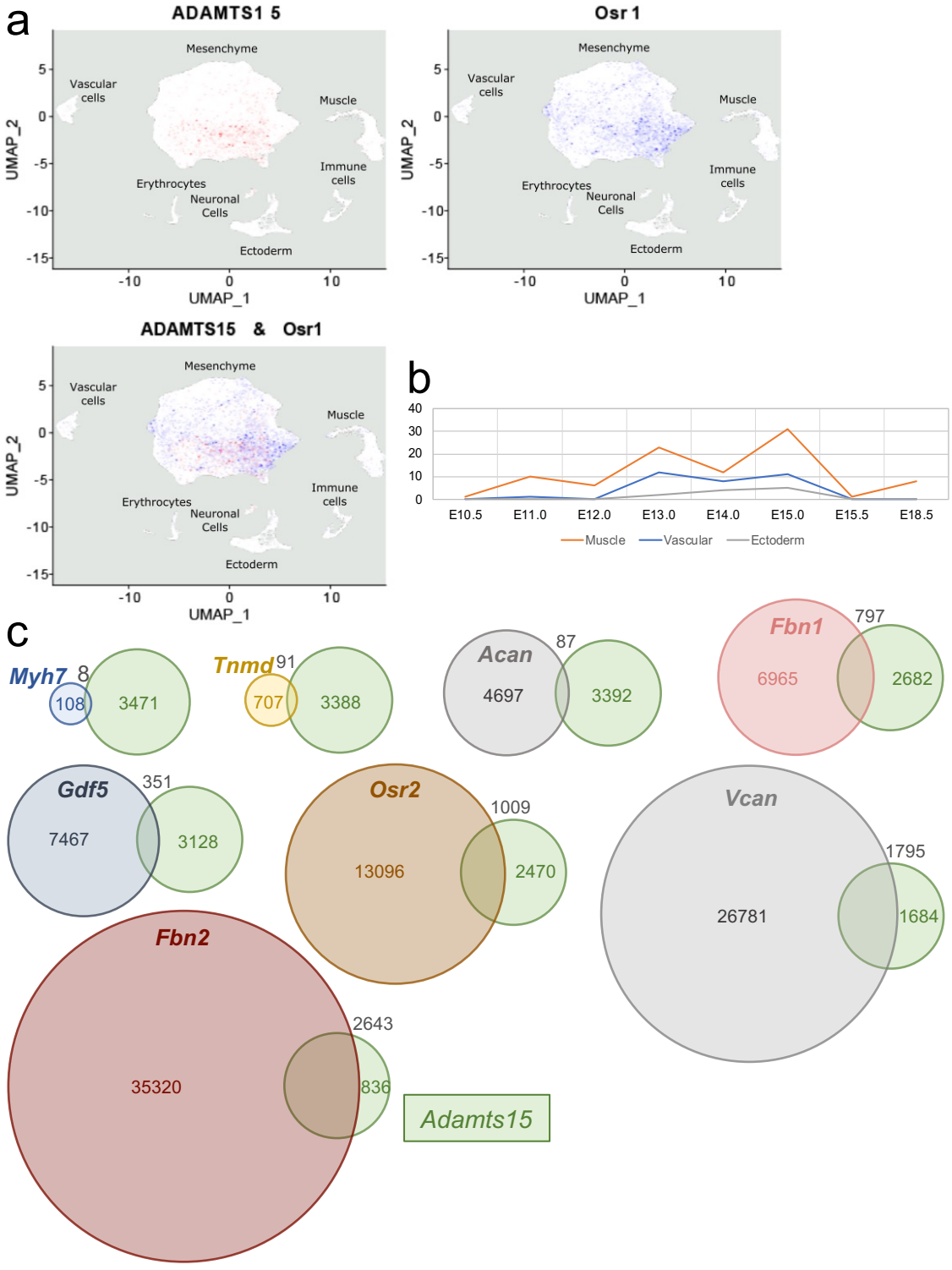

Figure S5. (a) Analysis of *Adamts15* and *Osr1* expression on single-cell level from whole embryo single-cell sequencing data. (b) Single-cell analysis of *Adamts15*-expressing cells of ectodermal, muscular, and vascular origin in the developing limb. Note that cell counts are much lower than those for mesenchymal cells (Figure 2b). (c) Co-expression of *Adamts15* and additional markers for muscles (*Myh7*), joints (*Gdf5*), fibrillin-1 (*Fbn1*), fibrillin-2 (*Fbn2*), and the proteoglycans aggrecan (*Acan*) and versican (*Vcan*). *Osr2* is a marker for muscle connective tissue and early tendon progenitors with expression domains overlapping or adjacent with *Osr1*. *Tnmd* encodes for tenomodulin, a tendon marker.

Table S1. Clinical features of affected individuals with biallelic *ADAMTS15* pathogenic variants

	Family A		Family B	Family C	Family D
ID	Individual 1 (II-1)	Individual 2 (II-4)	Individual 3 (II-6)	Individual 4 (II-1)	Individual 5 (II-2)
Variant	c.123C>G; p.(Tyr41*)	c.123C>G; p.(Tyr41*)	c. 1903-2A>G p.(Val635Alafs*30)	c. 2281G>A; p.(Gly761Ser)	c.2715C>G; p.(Cys905Trp)
Zygosity	homozygous	homozygous	homozygous	homozygous	homozygous
Gender	male	male	female	male	male
Familial History and Perinatal Period					
Ancestry	Syria	Syria	Turkey	Kosovo	Turkey
Consanguinity	+	+	+	+	+
Pregnancy	prematurity (32 weeks)	unremarkable	unremarkable	unremarkable	oligohydramanion
Miscarriages	-	-	3	-	1
Growth Parameters and Development					
Birth length	N/A	N/A	50 cm (- 1.1 SD)	51 cm (- 0.7 SD)	47 cm (- 2.6 SD)
Birth weight	N/A	N/A	3000 g (- 1.2 SD)	3460 g (- 0.4 SD)	2725 (- 2.2 SD)
Head circumference at birth	N/A	N/A	35 cm (+ 0.1 SD)	34 cm (- 1.2 SD)	34.5 (- 1 SD)
Age at examination	17 y 5 m	9 y 7 m	17 y	3 y 1 m	8 y 7m
Height	163.5 cm (- 2.3 SD)	129 cm (-1.7 SD)	165 cm (- 0.5 SD)	96.2 cm (- 0.3 SD)	123 cm (- 1.6 SD)
Weight	67 kg (-0.3 SD)	26.4 kg (- 1.4 SD)	47 kg (- 1.7 SD)	14.0 kg (- 0.4 SD)	21.6 kg (- 3.1 SD)
Head circumference	N/A	51 cm (- 1.9 SD)	56 cm (+ 0.6 SD)	50.2 cm (- 0.4 SD)	52.5 cm (- 0.5 SD)
Psychomotor development	normal	normal	normal	normal	normal
Clinical Manifestations					
upper limbs/ hand					
Congenital finger flexion contractures (HP:0005879)	+	+	+	+	+
Absent/hypoplastic distal interphalangeal creases (HP:0001032)	+	+	+	+	+
Hand muscle atrophy (HP:0009130)	+	+	+	+	+
Tapered distal phalanges of finger (HP:0009884)	+	+	+	+	+
Clinodactyly of the 5th finger (HP:0004209)	+	+	+	+	+
Hypoesthesia (HP:0033748)	+	-	+	-	-
Palmar hyperhidrosis (HP:0006089)	-	+	+	-	-
Hand X-ray	normal	normal	normal	N/A	N/A
lower limbs/ feet					
Talipes equinovarus (HP:0001762)	+	-	-	-	-
Flexion contracture of toe (HP:0005830)	+	+	+	+	+
Achilles tendon contracture (HP:0001771)	+	+	-	(+)	(+)
Ankle flexion contracture (HP:0006466)	+	+	+	-	+
Knee flexion contracture (HP:0006380)	+	+	+	-	+
Acroparesthesia (HP:0031006)	+	-	N/A	-	-
Feet X-ray	Talipes equinovarus	normal	normal	N/A	normal
Craniofacial features					
Low-set ears (HP:0000369)	+	+	+	+	-
Hypertelorism (HP:0000316)	-	-	+	-	-
Strabismus (HP:0000486)	+	-	-	-	+
Ptosis (HP:0000508)	-	-	-	-	+
High palate (HP:0000218)	N/A	N/A	N/A	-	+
Dental anomalies	dental crowding	dental crowding	agenesis of two maxillary incisiors	-	dental crowding
Spine					
Scoliosis (HP:0002650)	+	+	+	-	-
Spinal rigidity (HP:0003306)	+	+	+	-	-
Thoracic kyphosis (HP:0002942)	+	+	(+)	-	+
Other findings					
	cryptorchidism, testosterone deficiency		inguinal hernia, mitral valve prolapse, dry skin, Von Willebrand disease	inguinal hernia, cryptorchidism, two pathological fractures	hydrocele testis

Abbreviations: + = present; - = absent; (+) = mild; N/A = not available, y = year; m = month, SD = standard deviation

Table S2. Comparison of the clinical findings of affected individuals carrying biallelic variants in *ADAMTS15* with the main features of different types of Weill-Marchesani syndrome (WMS), congenital contractural arachnodactyly (CCA, Beals syndrome) and geleophysic dysplasia 1 (GPHYSD1).

Disorder	**Reported here**	**WMS1**	**WMS2**	**WMS3**	**WMS4**	**CCA**	**GPHYSD1**
Phenotype MIM number		277600	608328	614819	613195	121050	231050
Gene	*ADAMTS15*	*ADAMTS10*	*FBN1*	*LTBP2*	*ADAMTS17*	*FBN2*	*ADAMTSL2*
Inheritance	AR	AR	AD	AR	AR	AD	AR
Musculoskeletal							
Short stature	-	+	+	+	+	-	+
Brachydactyly	-	+	+	+	(+)	-	+
Joint stiffness	+	+	+	+	-	+	+
Pseudomuscular build	-	+	+	-	+	-	-
Delayed bone age	+	+	+	-	-	-	+
Scoliosis	+	+	+	-	-	+	-
Talipes equinovarus	+	-	-	-	-	+	-
Eye anomalies							
Ectopia lentis	-	+	+	+	+	(+)	-
Microspherophakia	-	+	+	+	-	-	-
Glaucoma	-	+	+	+	+	(+)	-
Cataract	-	+	+	-	-	(+)	-
Strabismus	+	-	-	-	-	-	-
Myopia	-	+	+	+	+	+	-
Cardiovascular							
Aortic root dilation	-	-	(+)	-	-	(+)	-
Bicuspid aortic valve	-	-	-	-	-	(+)	-
Atrial septal defect	-	+	+	-	-	(+)	-
Aortic valve stenosis	-	+	+	+	-	-	+
Mitral valve prolapse	+	+	+	-	-	+	-
Ventricular septal defect	-	+	+	-	-	(+)	-
Craniofacial							
Abnormal shape of face	-	-	elongated	-	-	elongated	rounded
Low-set ears	+	-	-	-	-	-	-
Crumpled ears	-	-	-	-	-	+	-
Dental anomalies	+	+	+	-	-	-	-
Highly arched palate	-	-	-	-	-	+	-
Other							
Intellectual disability	-	(+)	(+)	-	-	-	(+)
Thickened skin	-	+	+	-	-	-	+
References	-	GeneReviews NBK1114, PMID 32290605, 22539340				PMID 20301560, 31316167	PMID 18677313

Abbreviations: + = present; - = absent; (+) = mild/rare; AR = autosomal recessive; AD = autosomal dominant

Table S3. Molecular data and in-silico prediction of *ADAMTS15* variants.

Family	A	A	B	C	D
Individual	1	2	3	4	5
Sex	male	male	female	male	male
Ethnicity/Anchestry	Syria	Syria	Turkey	Kosovo	Turkey
***ADAMTS15* (HGNC:16305; variant description, in silico prediction**					
gDNA (GRCh37; NC_000011.9)	g.130318991C>G	g.130318991C>G	g.130341101A>G	g.130343144G>A	g.130343578C>G
cDNA (NM_139055.3)	c.123C>G	c.123C>G	c.1903-2A>G	c.2281G>A	c.2715C>G
RNA	n.a.	n.a.	r.1903_2078del (Exon 7)	n.a.	n.a.
Protein (NP_620686.1)	p.(Tyr41*)	p.(Tyr41*)	p.(Val635Alafs*30)	p.(Gly761Ser)	p.(Cys905Trp)
Genotype	homozygous	homozygous	homozygous	homozygous	homozygous
Inheritance	recessive	recessive	recessive	recessive	recessive
gnomAD Frequency (v.2.1.1)	-	-	-	0.0000039 (1x het)	-
Mutation Taster	pathogenic	pathogenic	pathogenic	pathogenic	pathogenic
CADD (v1.6)	35	35	33	28,9	26,8
Metadome	n.a.	n.a.	n.a.	slighly intolerant (0.66);	intolerant (0.31)
Domain	Reprolysin family propeptide (PF01562) bzw. n.a.	Reprolysin family propeptide (PF01562) bzw. n.a.	n.a.	ADAMTS Spacer 1 (PF05986)	Thrombospondin Type 1 domain (PF00090)
ACMG Classification	PVS1, PM2, PP4	PVS1, PM2, PP4	PVS1, PM2, PP4	PM1_sup, PM2, PP3, PP4	PM1_sup, PM2, PP3, PP4

Legend: n.a. not applicable

Table S4. Absence of heterozygosity (AOH) at *ADAMTS15* locus and inbreeding coefficients

Family	A			B	D		
Individual	Individual II-1	Father	Mother	Individual II-6	Individual II-2	Father	Mother
Ethnicity/Anchestry	Syria	Syria	Syria	Turkey	Turkey	Turkey	Turkey
Parental relationship	First cousins			First cousins	First cousins		
AOH block surrounding variant	5.3 Mb	none	none	4.1 Mb	5.1 Mb	none	none
Total autosomal AOH	360.5 Mb	183.9 Mb	32.8 Mb	201.3 Mb	351.8 Mb	213.8 Mb	301.5 Mb
Estimated inbreeding coefficient	0.0625			0.0625	0.0625		
Calculated inbreeding coefficient	0.12	0.058	0.006	0.06	0.095	0.055	0.064